Molecular dynamics simulations of a flexible molecule in a liquid crystalline solvent

J. Alejandre, J. W. Emsley, D. J. Tildesley, and P. Carlson

Citation: The Journal of Chemical Physics **101**, 7027 (1994); doi: 10.1063/1.468328
View online: http://dx.doi.org/10.1063/1.468328
View Table of Contents: http://scitation.aip.org/content/aip/journal/jcp/101/8?ver=pdfcov
Published by the AIP Publishing

Molecular dynamics simulations of a flexible molecule in a liquid crystalline solvent

J. Alejandre,[a] J. W. Emsley, and D. J. Tildesley
Department of Chemistry, The University, Southampton SO17 1BJ, United Kingdom

P. Carlson
Department of Chemistry, University of California, Berkeley, California 94720

(Received 3 June 1994; accepted 7 July 1994)

Molecular dynamics simulations of a hexane molecule in isotropic, nematic, and smectic phases are reported. The interactions between the solvent molecules is modeled using the Gay–Berne potential and the hexane–solvent potential is modeled as an explicit site–site interaction. The conformational distributions are reported of the hexane molecule at a fixed temperature but at different densities in isotropic, nematic, and smectic phases, and these are compared with the results from Monte Carlo simulations on an isolated molecule at the same temperature. The positions and orientations of the hexane molecule at each time step in the molecular dynamics simulations are used to calculate interproton dipolar coupling constants. These data are used to test the mean field models which have been applied with dipolar couplings obtained previously from nuclear magnetic resonance (NMR) experiments to yield conformational distributions.

I. INTRODUCTION

Rotations about the C–C bonds in *n*-alkanes have low barriers ($\approx$12 kJ mol^{-1}), so that at temperatures in the region of 300 K the whole of the conformational space generated by multiple bond rotations is sampled by molecules in the gas or liquid phases. The rotational potential about each C_j-C_{j+1} bond has a minimum energy when the $C_{j+1}-C_{j+2}$ bond is rotated through $\phi=180°$ with respect to the $C_{j-1}-C_j$ bond (the *trans*, *t*, state), and there are two equal secondary minima when $\phi\approx\pm120°$ (the *gauche*$\pm$, $g\pm$, states). A simplified view of the conformations adopted by an *n*-alkane is that only *t* or $g\pm$ states exist for each bond, so that the conformations of *n*-hexane, for example, are represented as combinations *ttt*, *ttg*+, *ttg*−, etc., with the all trans, *ttt*, as the lowest in energy. In a gas at low pressure and high temperature there will be a negligible effect from intermolecular forces on the conformational distribution, but in a liquid phase at normal densities the close proximity of neighboring molecules may affect the distribution, favoring those conformations which have the smaller molar volumes. In the crystalline solid state the molecules are all in the all *trans* conformation.

Liquid crystalline phases are particularly intriguing in that molecular mean field theories predict that the orientational order in these phases can produce a change in a conformational distribution.[1] Conformers which enhance the anisotropy in the mean potential are favored over those that have the opposite effect. This effect has been predicted to produce changes in the population of individual conformers at the nematic–isotropic transition by as much as 30% in pure liquid crystals.[2] The molecular dynamics technique is a useful tool for studying these conformational changes in model systems and simulation results have already been reported for the nematic phase of 4,4′-*n*-pentyl-cyano bicyclohexane.[3]

The same phenomenon is expected for a solute dissolved in a liquid crystalline phase, although it is usually of smaller magnitude because of their orientational order is considerably less. This paper reports molecular dynamics simulations of a single hexane molecule dissolved in a model liquid crystalline solvent. The conformational order of the hexane is studied as the solvent changes from the isotropic to the nematic to the smectic *B* phase by increasing the density at constant temperature and from the nematic to the smectic *B* phase by decreasing the temperature at constant density.

The magnitude of these conformational changes can also be investigated using nuclear magnetic resonance (NMR) spectroscopy.[4–7] Thus, the dipolar couplings, D_{ij}, between the protons in a molecule in a liquid crystalline phase are averaged by the overall rotational and translational motion of the molecules, and also by any internal bond rotational motion. The resulting averaged coupling is given by

$$D_{ij}=-\gamma_i\gamma_j h\langle(3\cos^2\theta_{ij}-1)/r_{ij}^3\rangle/8\pi^2, \tag{1}$$

where γ_i and γ_j are the gyromagnetic ratios of the two interacting nuclei, r_{ij} is their separation, and θ_{ij} the angle that r_{ij} makes with the mesophase director $\hat{\mathbf{n}}$, which is assumed to be parallel to the applied magnetic field. The $\langle\ \rangle$ denotes motional averaging. Pines *et al.*[7] have obtained sets of D_{ij} for *n*-alkanes dissolved in a nematic liquid crystalline solvent, and they have derived conformational distributions from these by using molecular mean field models. The general procedure they adopt is to express the D_{ij} as

$$D_{ij}=\sum_n p(n)D_{ij}(n), \tag{2}$$

where $p(n)$ is the probability of the *n*th conformation in which the dipolar coupling has a value of $D_{ij}(n)$. For a single conformer the dipolar couplings $D_{ij}(n)$ are obtained

[a]Permanent address: Departmento de Quimica, Universidad Automona Metropolitana-Iztapalapa, Apdo. Postal 55-534, 09340 Mexico, D.F., Mexico.

 0021-9606/94/101(8)/7027/10/$6.00

using Eq. (1), but with the simplification that now r_{ij} is fixed for all proton pairs, that is, motion other than rotations about bonds is neglected, so that

$$D_{ij}(n) = -\gamma_i \gamma_j h \langle 3\cos^2\theta_{ij}(n) - 1\rangle / 8\pi^2 r_{ij}^3(n) \tag{3}$$

and

$$\langle 3\cos^2\theta_{ij}(n) - 1\rangle = Q(n)^{-1} \int [3\cos^2\theta_{ij}(n) - 1] \times \exp[-U_{\text{ext}}(\beta,\gamma,n)/kT] \sin\beta d\beta d\gamma. \tag{4}$$

$U_{\text{ext}}(\beta,\gamma,n)$ is a conformationally dependent potential of mean torque, with β and γ the polar and azimuthal angles that the mesophase director makes with reference axes fixed in the molecule, and $\theta_{ij}(n)$ is the angle between $r_{ij}(n)$ and the director. $Q(n)$ is an orientational partition function,

$$Q(n) = \int_0^{2\pi} d\gamma \int_0^{\pi} \sin\beta d\beta \exp[-U_{\text{ext}}(\beta,\gamma,n)/kT]. \tag{5}$$

The probabilities, $p(n)$ depend upon the total mean potential

$$U(\beta,\gamma,n) = U_{\text{ext}}(\beta,\gamma,n) + U_{\text{int}}(n), \tag{6}$$

where $U_{\text{int}}(n)$ is that part of the mean potential which depends on the conformational state, but not on the orientation of the molecule, and which does not vanish in the isotropic phase. For the *n*-alkanes $U_{\text{int}}(n)$ is assumed to be

$$U_{\text{int}}(n) = N_g E_{tg} + N_{g\pm g\mp} E_{g\pm g\mp}; \tag{7}$$

N_g is the number of gauche states in the conformer, E_{tg} is the difference in energy between the *trans* and *gauche* forms, $N_{g\pm g\mp}$ is the number of $g\pm g\mp$ sequences, which carry an extra energy of $E_{g\pm g\mp}$.

Pines *et al.*[7] tried different models for $U_{\text{ext}}(\beta,\gamma,n)$, and fitted the calculated to the observed couplings by adjusting the disposable parameters defining $U(\beta,\gamma,n)$. Note that these mean field models predict that $p_{\text{LC}}(n)$, the conformational probability in the liquid crystalline phase, differs from $p_{\text{iso}}(n)$, the value for the isotropic phase at the same temperature and density. Thus,

$$p_{\text{LC}}(n) = Q(n) Z^{-1} \exp[-U_{\text{int}}(n)/kT], \tag{8}$$

with

$$Z = \sum_n \int_0^{\pi} \exp[-U(\beta,\gamma,n)/kT] \sin\beta d\beta \tag{9}$$

and,

$$p_{\text{iso}} = \frac{\exp[-U_{\text{int}}(n)/kT]}{\sum_n \exp[-U_{\text{int}}(n)/kT]}. \tag{10}$$

The extent to which these two probabilities differ depends upon the relative magnitudes of $U_{\text{ext}}(\beta,\gamma,n)$ and $U_{\text{int}}(n)$, and so is dependent on the models chosen for both potentials. The molecular dynamics technique affords an excellent opportunity to test these procedures for obtaining conformational probabilities from the NMR experimental results. To do this we have simulated the dynamics of *n*-hexane dissolved in a liquid crystalline solvent, and calculated a set of dipolar couplings, $D_{ij}(\text{sim})$. These couplings correspond to a known conformational distribution, i.e., that calculated directly in the simulation. The simulated couplings are then used in place of experimentally observed couplings in the mean field treatments, to yield conformational distributions which can be compared with the simulated distribution.

The liquid crystalline solvent used in the experiments[7] was *p*-pentylphenyl-2-chloro-4-(*p*-pentylbenzoyloxy)-benzoate, and it is impracticable to attempt a molecular dynamics simulation of such a large molecule, and so we have used a simpler solvent. In fact, since our aim is primarily to investigate a general phenomenon, that is the effect that any liquid crystalline solvent has on the conformations of a flexible molecule, and also to test a general procedure used to derive information from experimentally obtained dipolar couplings, rather than to attempt to reproduce a particular experimental result, we can chose any convenient solvent. In this case we have chosen the simplest possible solvent, one comprised of rigid spherocylinders interacting with each other with the potential developed by Gay and Berne.[8] A phase diagram produced from simulations on collections of these particles has been published,[9] and it is possible to choose the density and temperature so as to produce isotropic, nematic or smectic *B* phases. The interaction of a single *n*-hexane molecule dissolved in the Gay–Berne solvent is modeled as between united CH_2 or CH_3 atoms on the solute and four equally spaced Lennard-Jones centers on each solvent particle. Simulations on benzene in such a solvent have shown that this model does produce results which have the same general features as those for solutes in real liquid crystalline solvents.[10]

II. THE POTENTIAL MODEL

A. The solvent–solvent interaction

The interaction between two solvent molecules is modeled using the Gay–Berne potential; a Lennard-Jones-type interaction with orientation dependent range and well-depth parameters,[8]

$$U(\hat{\mathbf{u}}_1,\hat{\mathbf{u}}_2,\hat{\mathbf{r}}) = \epsilon_0 \epsilon_1^{\nu} \epsilon_2^{\mu} (\hat{\mathbf{u}}_1,\hat{\mathbf{u}}_2,\hat{\mathbf{r}})(R^{-12} - R^{-6}). \tag{11}$$

The $\hat{\mathbf{u}}_1$ and $\hat{\mathbf{u}}_2$ are unit vectors along the symmetry axes of the particles, and R is a reduced and shifted distance parameter related to the vector, $\mathbf{r}$, between the centers of mass of two Gay–Berne particles. The function ϵ_1 is

$$\epsilon_1(\hat{\mathbf{u}}_1,\hat{\mathbf{u}}_2) = [1 - \chi^2(\hat{\mathbf{u}}_1,\hat{\mathbf{u}}_2)]^{-1/2}, \tag{12}$$

where

$$\chi = \frac{[(\sigma_{\parallel}/\sigma_{\perp})^2 - 1]}{[(\sigma_{\parallel}/\sigma_{\perp})^2 + 1]}. \tag{13}$$

The function ϵ_2 is

$$\epsilon_2(\hat{\mathbf{u}}_1,\hat{\mathbf{u}}_2,\hat{\mathbf{r}})=1-\frac{\chi'}{2}\left[\frac{(\hat{\mathbf{u}}_1\cdot\hat{\mathbf{r}}+\hat{\mathbf{u}}_2\cdot\hat{\mathbf{r}})^2}{1+\chi'(\hat{\mathbf{u}}_1\cdot\hat{\mathbf{u}}_2)}+\frac{(\hat{\mathbf{u}}_1\cdot\hat{\mathbf{r}}-\hat{\mathbf{u}}_2\cdot\hat{\mathbf{r}})^2}{1-\chi'(\hat{\mathbf{u}}_1\cdot\hat{\mathbf{u}}_2)}\right], \tag{14}$$

where

$$\chi'=\left[\frac{(\epsilon_\perp/\epsilon_\parallel)^{1/\mu}-1}{(\epsilon_\perp/\epsilon_\parallel)^{1/\mu}+1}\right]. \tag{15}$$

The subscripts $\parallel$ and $\perp$ refer to the orientations of the particle axes relative to the interparticle vector, $\mathbf{r}$. The reduced and shifted distance parameter R is defined as

$$R=[r-\sigma(\hat{\mathbf{u}}_1,\hat{\mathbf{u}}_2,\mathbf{r})+\sigma_0]/\sigma_0. \tag{16}$$

with

$$\sigma_0=\sigma_\perp \tag{17}$$

and

$$\sigma(\hat{\mathbf{u}}_1,\hat{\mathbf{u}}_2,\hat{\mathbf{r}})=\sigma_0\left\{1-\frac{\chi}{2}\left[\frac{(\hat{\mathbf{u}}_1\cdot\hat{\mathbf{r}}+\hat{\mathbf{u}}_2\cdot\hat{\mathbf{r}})^2}{1+\chi(\hat{\mathbf{u}}_1\cdot\hat{\mathbf{u}}_2)}+\frac{(\hat{\mathbf{u}}_1\cdot\hat{\mathbf{r}}-\hat{\mathbf{u}}_2\cdot\hat{\mathbf{r}})^2}{1-\chi(\hat{\mathbf{u}}_1\cdot\hat{\mathbf{u}}_2)}\right]\right\}^{-1/2}. \tag{18}$$

This potential was originally proposed to mimic the interaction between two molecules composed of four equally spaced, collinear Lennard-Jones sites separated by $2\sigma_0/3$. A number of simulations have been performed of this model.[9,11–13]

In this work we use the same parameters as de Miguel *et al.*,[9] $\nu=1$, $\mu=2$, $\sigma_\parallel/\sigma_\perp=3$, $\epsilon_\parallel/\epsilon_\perp=1/5$. An approximate phase diagram for this model has been determined by simulation.

It is necessary to estimate the parameters σ_0 and ϵ_0 in the GB potential to obtain a reasonable approximation to the solute–solvent interaction. In this work the parameters for the solvent are estimated by considering a typical mesogen 4,4′-dimethoxyazoxybenzene (PAA). The experimental nematic–isotropic transition temperature for PAA is 407 K at ambient pressure. The model phase diagram for the Gay–Berne potential[9] indicates that $T^*_{\mathrm{NI}}=1.0$ for $\rho^*=0.32$ and that the transition temperature is not a strong function of density; a comparison of the experimental and model gives $\epsilon_0/k_B=407$ K. The value of σ_0 is estimated from the length of the PAA molecule; that is the distance between the outside edge of the terminal methyl group. This distance of 17.1 Å is estimated from a molecular model[14] and is equivalent to $3\sigma_0$, giving $\sigma_0=5.7$ Å. It should be stressed that these are approximate estimates of the solvent parameters and that small changes in these values are unlikely to affect the conformational distribution of the solute.

B. The intramolecular potential for hexane

The simulated fluid contains only one hexane molecule and thus only the intramolecular interactions are considered. Hexane is modeled using six equivalent united atoms representing the methyl and methylene groups.

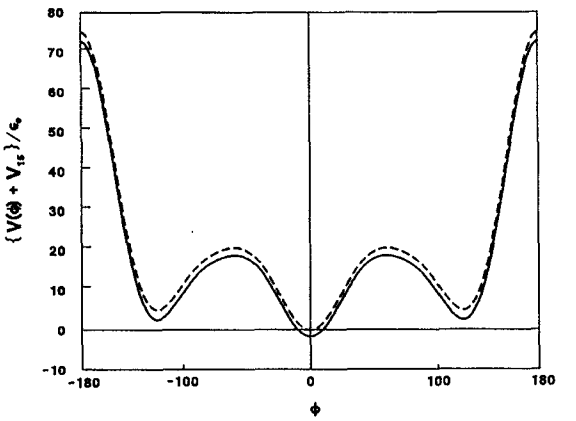

FIG. 1. The torsional potential for an isolated hexane molecule. The dotted line is the Rykaert and Bellemans torsional potential, $V(\phi)$, of Eq. (20). The solid line is the potential $V(\phi)+V^{15}_{\mathrm{LJ}}+V^{16}_{\mathrm{LJ}}+V^{26}_{\mathrm{LJ}}$ for the rotations around ϕ_1, ϕ_2, and ϕ_3 with $\phi_{j\neq i}=0°$. The three curves are indistinguishable on this scale.

The bond lengths in the hexane molecule are constrained at their equilibrium values of 1.53 Å. The bond angles, θ_i between two adjacent carbon–carbon bonds, are controlled by harmonic potentials of the form

$$V(\theta_i)=k_\theta[1-\cos(\theta_i-\theta_0)], \tag{19}$$

where $\theta_0=112°$ is the equilibrium bond angle and the constant $k_\theta=520$ kJ mol^{-1}.

The three torsional potentials are taken to be equivalent and have the functional form suggested by Rykaert and Bellemans,[15]

$$V(\phi_i)=\sum_{i=0}^{5} c_i\cos^i(\phi_i) \tag{20}$$

with c_0/kJ mol^{-1}=9.278, c_1/kJ mol^{-1}=12.16, c_2/kJ mol^{-1} =−13.12, c_3/kJ mol^{-1}=−3.060, c_4/kJ mol^{-1}=26.24, c_5/kJ mol^{-1}=−31.49. The mass of the hexane molecule is divided equally between each site. The minima in this potential are at $\phi=0°$ and $\pm120°$, and the difference in energy, E_{tg}, is 2.927 kJ mol^{-1}. The shape of this potential is shown in Fig. 1, and is the same for rotations about the three bonds C_2–$C_3[V(\phi_1)]$, C_3–$C_4[V(\phi_2)]$, and C_4–$C_5[V(\phi_3)]$.

The nonbonded or 1-5 interaction between sites in the same molecule is represented by a Lennard-Jones potential with energy and length parameters; $\sigma_{\mathrm{MeMe}}=3.923$ Å and $\epsilon_{\mathrm{MeMe}}/k_B=72$ K.[15] The variation in the Lennard-Jones potential with the angles ϕ_i, in each case with $\phi_{j\neq i}=0°$, is shown in Fig. 2. This potential is the sum of the 1-5, 1-6, and 2-6 interactions. The figure demonstrates that the nonbonded interactions make the inner and outer bond rotational potentials different. This difference is, however, very small, as shown in Fig. 1, where the total potentials for bond rotation are shown, again for the case that $\phi_{j\neq i}=0°$. The effect of including the Lennard-Jones terms is to lower the energy of the *gauche* forms relative to the *trans* by 0.573 kJ mol^{-1}, so that E_{tg} becomes 2.354 kJ mol^{-1}.

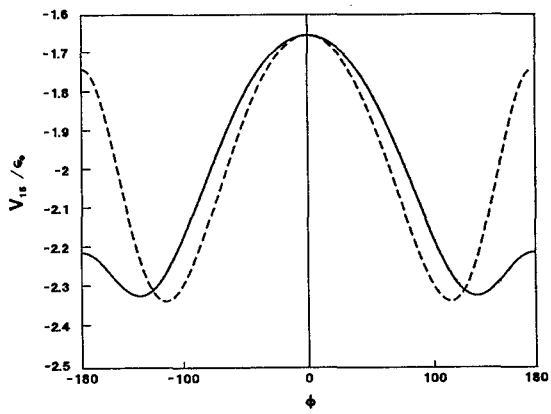

FIG. 2. The nonbonded potential for an isolated hexane molecule, $V_{LJ}^{15}+V_{LJ}^{16}+V_{LJ}^{26}$, as a function of the dihedral angle, ϕ_i. Solid line ϕ_1 varies with $\phi_2=\phi_3=0°$ (an identical curve is obtained as ϕ_3 varies with $\phi_1=\phi_2=0°$). Dashed line ϕ_2 varies with $\phi_1=\phi_3=0°$.

C. The solute–solvent interaction

The solvent molecules interact with each other through the Gay–Berne potential but the united atoms of the hexane molecule see the solvent as rigid linear molecules composed of four Lennard-Jones sites separated $2\sigma_0/3$.

The parameters describing the solute–solvent interaction are obtained using the normal mixing rules,

$$\sigma_{\mathrm{MeGB}}=\frac{\sigma_{\mathrm{MeMe}}+\sigma_{\mathrm{GBGB}}}{2}, \quad \epsilon_{\mathrm{MeGB}}=(\epsilon_{\mathrm{MeMe}}\epsilon_{\mathrm{GBGB}})^{1/2}. \quad (21)$$

The energy and length parameters of the interaction sites on the Gay–Berne molecule are $\sigma_{\mathrm{GB}}=1.05\sigma_0$ and $\epsilon_{\mathrm{GB}}=0.2\epsilon_0$. These parameters are chosen to provide a reasonable fit between the Gay–Berne potential and the corresponding four site Lennard-Jones potential. The quality of the fit is shown in Fig. 3 where both potentials are plotted as a function of the intermolecular separation for relative orientations: parallel; end to end; crossed and T configurations.

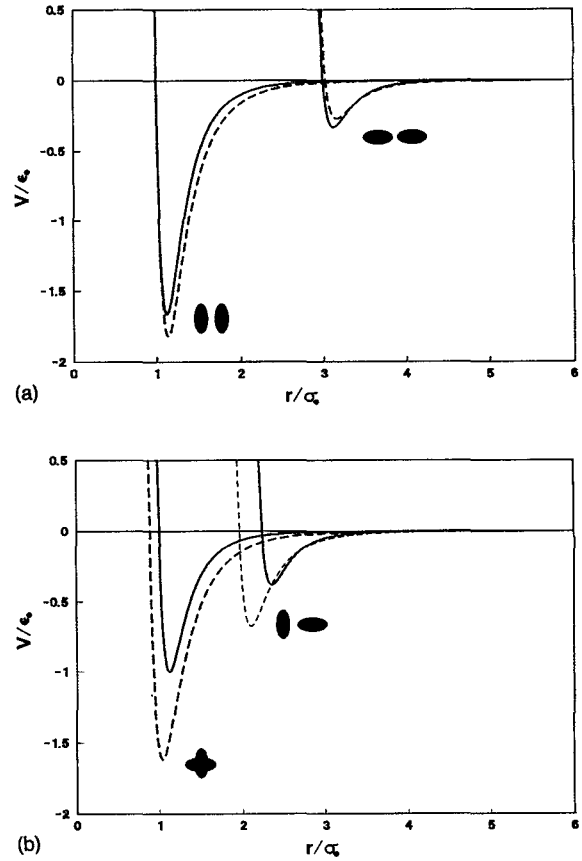

FIG. 3. The potential of two GB molecules as a function of the intermolecular separation r. The solid line is the full GB potential as given in Eq. (1). The dashed line is the approximation of the GB potential as four collinear Lennard-Jones sites using the parameters discussed in Sec. II C. (a) Parallel and end-to-end orientations; (b) crossed and T orientations.

III. THE MOLECULAR DYNAMICS SIMULATION

Molecular dynamics simulations have been performed for one hexane molecule in a solvent of 256 Gay–Berne molecules. Simulations were performed at a reduced temperature $T^*=k_BT/\epsilon_0=1.2$ and at reduced densities, $\rho^*=\rho\sigma_0^3=0.15$, 0.34, and 0.38. These three states are in the isotropic, nematic, and smectic phases of the solvent, respectively. In addition for the nematic phase at $\rho^*=0.34$, the temperature was reduced to $T^*=0.5$, which also takes the solvent into its smectic phase. Initially, the centers of mass of the Gay–Berne molecules were placed on a fcc lattice with the molecules perfectly aligned parallel to the diagonal of the simulation box. The hexane molecule was inserted at a random position in the solvent with the C_1–C_6 axis parallel to the solvent molecules. Initially, the potential between the solvent site and the united atom site in hexane was modified when the sites were significantly overlapped in the initial configuration. In this case a potential of the form

$$u_{\mathrm{overlap}}(r)=A\cos\left[\frac{\pi}{2}\left(\frac{r}{\sigma_{\mathrm{MeGB}}}\right)\right] \quad r<\sigma_{\mathrm{MeGB}}$$
$$=0 \quad r>\sigma_{\mathrm{MeGB}} \quad (22)$$

was used.

Initially the value of A was set to $500\epsilon_0$ and this value was used throughout the initial phase of the equilibration until all of the significant overlaps were removed. At this point the potential was reset to the Lennard-Jones form and the equilibration continued. The velocities of the molecules were chosen randomly from a Maxwell–Boltzmann distribution at the appropriate temperature and the net momentum in each of the three coordinate directions was set to zero. Normal periodic boundary conditions are used throughout the simulation.

The translational equations of motion of the Gay–Berne molecules were solved using the Verlet algorithm and the rigid-body rotational equations were solved using the method of Singer *et al.*[16] The equations of motion of the united atoms in the hexane molecule were solved using constraint dynamics with the SHAKE algorithm.[17]

A reduced time step of $\delta t^*=\delta t(\epsilon_0/m\sigma_0^2)^{1/2}=0.002$ was used throughout the calculation. Following previous

TABLE I. The orientational order parameter $\bar{P}_2$ for the four simulations reported in this paper.

ρ^*	T^*	$\bar{P}_2$	
0.15	1.2±0.02	0.060±0.001	isotropic
0.34	1.2±0.02	0.753±0.003	nematic
0.38	1.2±0.02	0.871±0.001	smectic
0.34	0.5±0.01	0.931±0.001	smectic

studies of the GB potential,[11] a reduced moment of inertia, $I^*=I/m\sigma_0^2=4$, was used to solve the rotational equations of motion. This choice does not affect the static properties described in this paper. The total energy is conserved to better than 1 part in 10^4 over 10^4 time steps.

During the equilibration period of 50×10^3 time steps, the velocities were rescaled every 20th time step to achieve the required temperature. The production phase of the simulation was performed at constant total energy. The averages were calculated over runs of 10^6 time steps, and the errors in the averages estimated by dividing the runs into 20 equal blocks and averaging these separately. The translational and rotational temperatures of the solvent and the temperature of the solute molecule were monitored independently. In each case these temperatures were equal to within the estimated error.

IV. THE RESULTS

The order parameter $\bar{P}_2$ was obtained for the solvent molecule by calculating the largest positive eigenvalue of the Q tensor for a particular configuration and averaging over the simulation. An element of the tensor is defined as

$$Q\alpha\beta=\frac{1}{2N}\left\langle\sum_{i=1}^{N}(3\mathbf{e}_{i\alpha}^{s}\mathbf{e}_{i\beta}^{s}-\delta_{\alpha\beta})\right\rangle, \tag{23}$$

where $\mathbf{e}_{i\alpha}^{s}$ is the αth component of the vector $\mathbf{e}_i^s$ defining the direction of the long-axis of molecule i in the space-fixed system. The instantaneous director is the eigenvector corresponding to the largest eigenvalue of Q. The order parameters are given in Table I. The simulation at $\rho^*=0.34$ and 0.38 correspond to liquid crystalline phases. An examination of the density distribution of the center of mass of the GB molecules in slices perpendicular to the director indicates that the first of these states is nematic and the second is a smectic B confirming the results of de Miguel *et al.*[9]

A. Conformations of the hexane molecule

The conformational probabilities of the hexane molecule at constant temperature in the three liquid phases are presented in Table II. The error analysis indicates that the populations are accurate to ±1%. The model shows very little change in the conformational distribution in moving from the isotropic to the smectic phase by varying the density at constant temperature. Certainly the results for the smectic and nematic phases are indistinguishable with the accuracy which can be achieved with runs of 10^6 time steps. There is a slight increase in the number of all-*trans* conformations as the system moves from the isotropic to the nematic phase,

TABLE II. The conformational distribution for the hexane molecule in a GB solvent as a function of density and temperature. $(\bar{P}_2)_{\text{hex}}$ is a measure of the orientational order of the hexane molecule.

	ttt	*ttg*	*tgt*	*tgg*	*gtg*	*ggg*	$(\bar{P}_2)_{\text{hex}}$
Isotropic ($T^*=1.2$)	19	34	18	12	15	2	0.03
Nematic ($T^*=1.2$)	21	33	17	10	16	3	0.24
Smectic *B* ($T^*=1.2$)	21	32	19	10	16	2	0.38
Smectic *B* ($T^*=0.5$)	65	14	18	0.6	2.4	0	0.73
Experiment nematic[a]	37	29	17	8	9	0	0.21
Ideal gas ($T^*=1.2$)	22	37	17	9	14	1	
Ideal gas ($T^*=0.5$)	44	34	14	2	7	0	

[a]Reference 19.

but this is only just statistically significant within our calculations. This phase independence of the conformation at constant T is presumably because there are two competing factors affecting the conformational distributions. An increase in the anisotropic environment will favor conformations such as the all-*trans*, but an increase in density will favor conformations with a minimum molar volume, such as those with more globular shapes by virtue of having more *gauche* links.

The overall ordering of the hexane molecule has been measured in the simulation by calculating $(\bar{P}_2)_{\text{hex}}$ which measures the ordering of the central C–C bond of the hexane with respect to the solvent director. As expected the hexane is not orientationally ordered in the isotropic phase of the solvent. Hexane in the nematic phase has $(\bar{P}_2)_{\text{hex}}$ about a third of $(\bar{P}_2)_{\text{GB}}$, that for the solvent molecules. There is a significant increase in the orientational ordering of hexane in the smectic phase where $(\bar{P}_2)_{\text{GB}}/(\bar{P}_2)_{\text{hex}}\simeq2.3$. The insensitivity of the conformational distribution of hexane to the orientational ordering of the liquid phase at a constant T^* of 1.2 is confirmed in Fig. 4 which shows the distribution of torsional angles, $n(\phi)$; all of the three torsional angles are included in this average. The distributions are indistinguishable on the scale of the plot.

The ideal gas values included in Table II were calculated using a Monte Carlo simulation of an isolated hexane molecule. Ten runs of 10^6 trial configurations were performed at each temperature using the flexible model of the hydrocarbon chain, i.e., without the metric tensor correction. The program was checked by reproducing the results of Almarza *et al.*[18] for the ideal gas hydrocarbons to within the estimated error of both simulations. The conformational distribution in all of the liquid phases at $T^*=1.2$ is similar to that for the hexane molecule in the ideal gas at the same temperature. There is a small decrease in the average number of conformations with two or more gauche states in moving from the liquid to the ideal gas but the differences are not dramatic.

The effect of temperature at constant density on the conformation of the hexane can be seen by comparing the simulations at $\rho^*=0.34$ as the temperature changes from

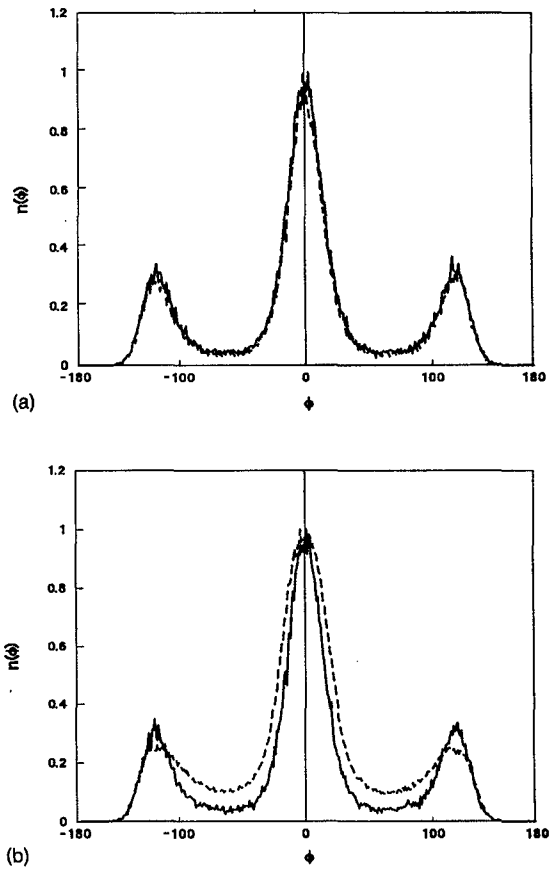

FIG. 4. The probability distribution $n(\phi)$ averaged over the three torsional potentials of hexane in a number of solvents at $T^*=1.2$. (a) In the isotropic phase $\rho^*=0.15$ (solid line) and in the nematic phase, $\rho^*=0.34$ (dashed line); (b) in the smectic B phase, $\rho^*=0.38$ (solid line) and in the ideal gas (dashed line).

$T^*=1.2$ to $T^*=0.5$. There is a sharp increase in the second rank order parameter of the hexane from 0.38 to 0.73 and the percentage of time the molecules spends in the all-*trans* conformation increases dramatically from 21% to 65%. At the lower temperature the percentage of conformations containing more than one gauche bond falls to approximately 3%. The effect of the fall of the temperature on the conformational distribution is reinforced by the phase transition from the nematic to the smectic phase. The lower temperature and the high degree of orientational ordering at the same density generate the large increase in the number of all-*trans* configurations. The importance of the phase transition and the resulting smectic ordering of the solvent can be seen by considering the ideal gas results at $T^*=0.5$. The ideal gas result shows the enhancement of the all-*trans* conformation due to the fall in the temperature, which changes from 22% to 44% as T^* is reduced from 1.2 to 0.5. The high degree of orientational ordering in the smectic phases further enhances the percentage of the all-*trans* configuration to 65%. Interestingly, the solvent order parameters of the smectic B phases at $T^*=1.2$ and $T^*=0.5$ are quite close to one another; $(\bar{P}_2)_{GB}=0.871$ $(\bar{P}_2)_{GB}=0.931$. However the hexane order parameters at these two points in the same phase are quite different; $(\bar{P}_2)_{hex}=0.38$ $(\bar{P}_2)_{hex}=0.73$, respectively.

TABLE III. The percentage of *trans* conformations for each independent torsional angle of hexane in the four mesophase simulations.

ϕ	Isotropic	Nematic	Smectic ($T^*=1.2$)	Smectic ($T^*=0.5$)
1	59.1±1.0	58.4±0.9	60.5±1.2	88±3
2	68.3±1.2	69.5±1.3	69.7±1.4	83±5
3	61.1±1.8	61.8±0.9	60.7±1.0	91±3

We can analyze the conformational distribution more closely by considering the percentage of *trans* conformers for the three independent torsional potentials. These are reported in Table III. These measurement give some indication of the accuracy with which we can measure these conformational distributions since the percentage of *trans* for bonds 1 and 3 should be the same by symmetry. For the isotropic and smectic phases these averages are the same within one standard deviation. For the nematic phase the agreement is slightly poorer with the average equal to within two standard deviations. It is clear that the conformation of the central torsion of the hexane is more likely to be in a *trans* configuration than the outer torsional angles. These results confirm the equivalence of the conformational behaviour within the three phases to within the simulation errors.

B. Calculation of dipolar couplings

As discussed in the Introduction, experimental measurements of the conformational distributions in the phases are obtained by fitting models to the interproton dipolar coupling constants. The values of the $D_{ij}(t)$ can be obtained at each time step from Eq. (1), but this requires the positions of the protons. These were obtained from the positions of the carbons by a simple geometrical construction. The plane HC_iH in each methylene group is perpendicular to the plane $C_{i-1}C_iC_{i+1}$. The C_iH bond lengths are fixed at their equilibrium value of 1.09 Å and the HC_iH bond-angles are fixed at 109.24°.

The labeling of the protons is shown in Fig. 5. The distance between the protons within each methyl group were determined by adopting a tetrahedral geometry with a *CH* bond length of 1.09 Å. This is all the geometrical information required in order to calculate the dipolar coupling between the protons within a methyl group, with the additional assumption that these protons rotate about the C–C bond as a rigid group, thus preserving the threefold symmetry about this direction. The averaging produced by the methyl group rotation on the intramethyl coupling is simply

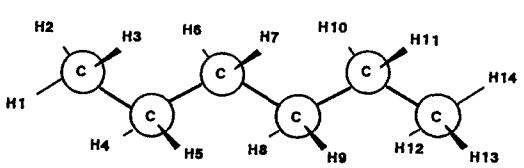

FIG. 5. The geometry of the hexane molecule corresponding to the dipolar couplings discussed in Sec. IV.

TABLE IV. Average dipolar coupling constants in each phase. The equivalences discussed in the text are used in these calculations.

D_{ij}/Hz	Isotropic	Nematic	Smectic ($T^*=1.2$)	Smectic ($T^*=0.5$)
$D_{1,2}$	35±46	1285±68	1768±85	4792±334
$D_{4,5}$	76±87	2892±137	4551±157	9115±341
$D_{4,6}$	9±21	93±33	49±33	805±105
$D_{4,7}$	10±27	59±44	−41±55	957±172
$D_{4,8}$	−27±23	−942±50	−1504±63	−4268±322
$D_{4,9}$	−43±20	−772±39	−1229±52	−1899±120
$D_{4,10}$	−7±18	−453±31	−696±32	−700±80
$D_{4,11}$	−28±22	−581±41	−891±49	−1330±321
$D_{6,7}$	37±93	3271±130	5219±169	9708±281
$D_{6,8}$	2±1	−14±28	78±30	13±194
$D_{6,9}$	1±26	−131±40	−84±49	−389±228

TABLE V. D_{ij} for hexane in the nematic phase. The results of the simulation are compared with two experiments. In comparing with the experiment the MD results have been scaled to match the experimental values of $D_{1,2}$.

	MD	Expt. A[a]	MD scaled	Expt. B[b]	MD scaled
$D_{1,2}$	1285±68	1876±28	1876	1526 ± 25	1526
$D_{4,5}$	2892±137	3974±34	4222	3288	3441
$D_{4,6}$	93±33	186±14	136		
$D_{4,7}$	59±44	81±12	86		
$D_{4,8}$	−942±50	−1616±25	−1375	−1323	−1120
$D_{4,9}$	−772±39	−1086±27	−1127	−881	−919
$D_{4,10}$	−453±31	−609±14	−661		
$D_{4,11}$	−581±41	−713±18	−848		
$D_{6,7}$	3271±130	4487±34	4776	3711	3893
$D_{6,8}$	−14±28	43±12	−20		
$D_{6,9}$	−131±40	−190±12	−191		

[a]Reference 19.
[b]Reference 7.

$$D_{12}=D_{13}=D_{23}=\tfrac{1}{3}[D_{12}(n)+D_{13}(n)+D_{23}(n)].$$

To calculate the couplings from the methyl protons to other protons in the molecule would require an additional assumption about the rotational potential, and so has not been attempted.

The symmetry of the hexane means that a number of the dipolar couplings are equivalent. The eleven independent coupling constants are

$$D_{1,2}=D_{1,3}=D_{2,3}=D_{12,13}=D_{12,14}=D_{13,14},$$

$$D_{4,5}=D_{10,11},$$

$$D_{6,7}=D_{8,9},$$

$$D_{4,8}=D_{5,9}=D_{6,10}=D_{7,11},$$

$$D_{4,9}=D_{5,8}=D_{6,11}=D_{7,10},$$

$$D_{4,10}=D_{5,11},$$

$$D_{4,11}=D_{5,10},$$

$$D_{4,6}=D_{5,7}=D_{8,10}=D_{9,11},$$

$$D_{4,7}=D_{5,6}=D_{8,11}=D_{9,10},$$

$$D_{6,8}=D_{7,9},$$

$$D_{6,9}=D_{7,8}.$$

The independent D_{ij} calculated in the simulation are given in Table IV. As expected the coupling constants for the isotropic phase are close to zero within the estimated error. The coupling constants in the mesophases are nonzero with those for the smectic phase larger in absolute magnitude than those in the nematic phase, indicating the increasing orientational ordering of the hexane in the smectic. These coupling constant can be compared directly with two sets of experimental measurements [*A* (Ref. 19) and *B* (Ref. 7).] We can scale the experimental results so that the simulated and experimental $D_{1,2}$ constants are identical. The scaling factors are 1.46 for experiment *A* and 1.19 for experiment *B* and these scaled results are given in columns 5 and 7 of Table V.

The scaled, simulated D_{ij} are in close agreement with the experimental data, which demonstrates that the simulations are producing results which are similar to those of real systems. Exact agreement is not expected since the orientational order of solutes varies with the nature of the real liquid crystalline solvents. In addition, the simulations do not include all the internal degrees of motional freedom.

C. Testing the methods of obtaining conformational distributions from experimental dipolar coupling data

Rosen *et al.*[7] analyzed their data with three methods for constructing $U_{\text{ext}}(\beta,\gamma,n)$. In each case the internal potential was approximated by the RIS model.

Model *A*, introduced by van Der Est *et al.*[20] treats the liquid crystal solvent as a continuum which is distorted by the solute. The potential of mean torque is

$$U^A_{\text{ext}}(\beta,\gamma,\phi)=kc^2(\beta,\gamma,n), \tag{24}$$

where c is the minimum circumference of the projection of the solute molecule on a plane containing the director; k measures the strength of the interaction of the solute with the solvent. The observed and calculated D_{ij} are brought into closest agreement by adjusting k and E_{tg}.

Models *B* and *C* both use an expansion for $U_{\text{ext}}(\beta,\gamma,n)$ in second-rank modified spherical harmonics, $C_{2,m}(\beta,\gamma)$,

$$U_{\text{ext}}(\beta,\gamma,n)=u_{2,0}(n)C_{2,0}(\beta,\gamma)+2u_{2,2}(n)C_{2,2}(\beta,\gamma), \tag{25}$$

where the $u_{2,m}(n)$ depend on the strength of the solute–solvent interaction. The conformational dependence of these coefficients is constructed in model *B* by the method proposed by Straley[21] for rigid molecules, and used by Janik, Samulski, and Toriumi[22] for nonrigid molecules, in which $u_{2,m}(n)$ depends on the length, L, the width, W, and breadth, B, of the solute,

$$u_{2,0}(n)=1/3\,\epsilon[6LBW+L(W^2+B^2)-2W(L^2+B^2)-2B(W^2+L^2)], \tag{26}$$

$$u_{2,2}(n)=\sqrt{6}\,\epsilon[(L^2-BW)(B-W)]. \tag{27}$$

The adjustable parameters are ϵ and E_{tg}.

Model *C* was introduced by Photinos, Samulski, and Toriumi,[23] and is based on the idea that the $u_{2,m}(n)$ can be

TABLE VI. Comparison of dipolar couplings calculated with model *C* with parameters optimized to fit data from experiments and simulation.

	Experiment		Simulation	
i,j	D_{ij}(obs)	D_{ij}(calc)	D_{ij}(sim)	D_{ij}(calc)
1,2	1526	1573	1285	1329
1,4	−310	−305		
1,6	−852	−901		
1,8	−484	−584		
1,10	−272	−273		
1,12	−167	−172		
4,5	3288	3172	2892	2734
4,6			93	76
4,7			59	140
4,8	−1323	−1440	−942	−1173
4,9	−881	−989	−772	−887
4,10			−453	−708
4,11			−581	−573
6,7	3711	3686	3271	3206
6,8			−14	−31
6,9			−131	66

constructed as a sum of contributions from molecular fragments. In the simplest version of this model the molecular fragments are identified as individual C–C bonds,[2,24] while Photinos *et al.*[23] introduced an additional contribution which differentiates between conformations which in the simplest model have identical potentials of mean torque although they have different shapes. This is done by including a contribution which depends on the relative orientation of adjacent bonds. The coefficients are obtained for a particular conformation by first constructing a Cartesian tensor **u**, in a reference frame *xyz* fixed in one rigid part of the molecule, which has elements,

$$u_{ab}=-\frac{2}{3}w_0\sum_{i=1}^{N}(3s_a^i s_b^i-\delta_{ab}\mathbf{s}^i\mathbf{s}^i)$$

$$-\frac{2}{3}w_1\sum_{i=1}^{N-1}[3(s_a^i s_b^{i+1}+\mathbf{s}^{i+1}\mathbf{s}^i)/2-\delta_{ab}\mathbf{s}^i\mathbf{s}^i], \qquad (28)$$

where N is the number of C–C bonds, $\mathbf{s}^i$ is a unit vector along the C_{i+1}–C_i bond with components s_a^i, and a is in turn x,y, and z. Diagonalizing **u** gives principal components u_{11}, u_{22}, and u_{33}, from which

$$u_{2,0}=1/\sqrt{6}[2u_{33}-(u_{11}+u_{22})], \qquad (29)$$

$$u_{22}=\tfrac{1}{2}(u_{11}-u_{22}). \qquad (30)$$

The adjustable parameters are w_1, w_2, and E_{tg}.

TABLE VII. Values of E_{tg} in kJ mol^{-1} obtained by fitting calculated to simulated dipolar couplings by the three theoretical models.

		E_{tg}		
T^*	Phase	*A*	*B*	*C*
1.2	nematic	4.61	3.97	2.45
1.2	smectic *B*	4.09	3.20	1.52
0.5	smectic *B*	3.49	3.56	2.60

TABLE VIII. Conformer populations (%) for *n*-hexane dissolved in the nematic phase of the Gay–Berne solvent at a scaled density of 0.34 and scaled temperature 1.2. derived by fitting the dipolar couplings D_{ij} calculated by the mean field methods of (*A*) van der Est *et al.* (Ref. 20), (*B*) Janik *et al.* (Ref. 22), and (*C*) Photinos *et al.* (Ref. 23), to those obtained from the computer simulation.

Isomer			*A*		*B*		*C*	
(degeneracy)	MD	Gas	$p_{LC}(n)$	$p_{iso}(n)$	$p_{LC}(n)$	$p_{iso}(n)$	$p_{LC}(n)$	$p_{iso}(n)$
ttt (1)	21	22	24	25	23	23	15	14
ttg± (4)	33	37	33	34	33	34	32	31
tg±*t* (2)	17	17	17	17	17	17	16	16
tg±*g*± (4)	10	9	12	11	12	12	16	17
tg±*g*∓ (4)			0.6	0.0	0.5	0.0	0.7	0.0
g±*tg*± (2)	16	14	6	6	6	6	8	9
g±*tg*∓ (2)			6	6	6	6	8	9
g±*g*±*g*∓ (4)	3	1	0.2	0.0	0.2	0	0	0
g±*g*∓*g*± (2)			0	0	0	0	0	0
g±*g*±*g*± (2)			2	2	2	2	4	5

As a test of these models they have been used with the D_{ij} obtained from the simulations to obtain E_{tg} and the conformer populations $p_{LC}(n)$ and $p_{iso}(n)$. Before discussing these values we note that the quality of the agreement between calculated and simulated D_{ij} is similar to that obtained by Rosen *et al.*[6] when comparing calculated and experimental couplings. Thus, Table VI shows the results of bringing values of D_{ij} calculated with model *C* into closest agreement with those observed, D_{ij}(exp), and a similar exercise involving simulated data, D_{ij}(sim). Note that exact agreement would not be expected for either D_{ij}(exp) or D_{ij}(sim) with D_{ij}(calc) since in each case the RIS model adopted for the conformational distribution is an approximation to the true distribution.

Values of E_{tg} obtained by each of the models *A*, *B*, and *C* from each of the three sets of simulated D_{ij} are given in Table VII. Their values determine $p_{iso}(n)$ through Eq. (10), and these populations are given in Tables VIII–X together with $p_{LC}(n)$.

It is interesting to note that a simple relationship does not exist between the closeness with which both E_{tg} and the conformer distributions are obtained. This is perhaps not surprising bearing in mind that the theoretical models use the RIS approximation for the conformer distribution, which means that only three points are being used to represent a continuous distribution in the rotational variables ϕ_i.

This is encouraging, but the data at this temperature do not provide a searching test for the models of $U_{ext}(\beta,\gamma,n)$ because the intermolecular potential has only a small effect on $p_{LC}(n)$. This can be seen by noting that $p_{LC}(n)$ is almost identical with $p_{iso}(n)$ and $p_{gas}(n)$, and it suggests that the analysis of NMR dipolar coupling constants obtained on samples of flexible molecules dissolved in real solvents, where the orientational order of the solute is usually similar to that found in the simulations at $T^*=1.2$, are almost independent of the model chosen for the potential of mean torque. It is important however, to use E_{tg} as an adjustable parameter.

The results obtained for the smectic phase at $T^*=0.5$ shown in Table X, show significant differences between each

TABLE IX. Conformer populations (%) for *n*-hexane dissolved in the smectic phase of the Gay–Berne solvent at a scaled density of 0.38 and scaled temperature 1.2. derived by fitting the dipolar couplings D_{ij} calculated by the mean field methods of (*A*) van der Est *et al.* (Ref. 20), (*B*) Janik *et al.* (Ref. 22), and (*C*) Photinos *et al.* (Ref. 23), to those obtained from the computer simulation.

Isomer (degeneracy)	MD	Gas	*A* $p_{LC}(n)$	*A* $p_{iso}(n)$	*B* $p_{LC}(n)$	*B* $p_{iso}(n)$	*C* $p_{LO}(n)$	*C* $p_{iso}(n)$
ttt (1)	21	22	21	23	20	18	13	10
$ttg\pm$ (4)	32	37	33	34	33	33	30	29
$tg\pm t$ (2)	19	17	16	17	16	16	15	14
$tg\pm g\pm$ (4)	10	9	13	12	13	15	17	20
$tg\pm g\mp$ (4)			0.6	0.0	0.3	0.0	0.7	0
$g\pm tg\pm$ (2)	16	14	7	6	7	7	9	10
$g\pm tg\mp$ (2)			7	6	7	7	9	10
$g\pm g\pm g\mp$ (4)	2	1	0.3	0.0	0.3	0.4	0	0
$g\pm g\mp g\pm$ (2)			0	0	0	0	0	0
$g\pm g\pm g\pm$ (2)			3	2	3	2	5	7

other, and they have important differences with the true distributions. Thus, although the models all obtain *ttt* as the most probable conformer, they underestimate its importance in both ordered and isotropic phases. The models all place $ttg\pm$ as the second most abundant, with about twice the population of $tg\pm t$ in third place. The real distribution has these two conformers in reverse order of abundance, and more nearly equal in population. The orientational order of the hexane in the S_B phase at $T^*=0.5$ is almost double that at $T^*=1.2$ in the same phase. It is the influence of the increased ordering which is now revealing differences between the populations derived from dipolar couplings and the simulated data. The theoretical models are clearly underestimating the importance of the intermolecular contribution to the mean potential.

Too much importance should not be attached to the closer agreement with the real distribution obtained by models *A* and *B* compared with *C*. The models use a discrete conformer distribution whereas the real distribution is continuous and includes more internal degrees of freedom. The models could be extended to sample more of the conformational space, and this might change their ability to reproduce the simulation data. In fact model *C* has been so extended and applied to the NMR data for *n*-hexane.[25] This lead to a much improved fit of calculated to observed dipolar couplings, and it certainly would be interesting to investigate whether such extended models could obtain better agreement between calculated and simulated data in the way explored here.

TABLE X. Conformer populations (%) for *n*-hexane dissolved in the smectic phase of the Gay–Berne solvent at a scaled density of 0.34 and scaled temperature 0.5 derived by fitting the dipolar couplings D_{ij} calculated by the mean field methods of (*A*) van der Est *et al.* (Ref. 20, (*B*) Janik *et al.* (Ref. 22), and (*C*) Photinos *et al.* (Ref. 23), to those obtained from the computer simulation.

Isomer (degeneracy)	MD	Gas	*A* $p_{LC}(n)$	*A* $p_{iso}(n)$	*B* $p_{LC}(n)$	*B* $p_{iso}(n)$	*C* $p_{LC}(n)$	*C* $p_{iso}(n)$
ttt (1)	65	44	52	53	59	54	47	37
$ttg\pm$ (4)	14	34	27	27	24	26	29	32
$tg\pm t$ (2)	18	14	14	13	12	13	15	16
$tg\pm g\pm$ (4)	0.6	2	4	3	2	3	5	7
$tg\pm g\mp$ (4)			0	0	0	0	0	0
$g\pm tg\pm$ (2)	2	8	2	2	1	2	2	3
$g\pm tg\mp$ (2)			2	2	1	2	3	4
$g\pm g\pm g\mp$ (4)	0	0	0	0	0	0	0	0
$g\pm g\mp g\pm$ (2)			0	0	0	0	0	0
$g\pm g\pm g\pm$ (2)			0	0	0	0	0	1

V. CONCLUSIONS

Our aim has been to show the usefulness of simulations of a flexible solute dissolved in a Gay–Berne solvent. The simulations show that there is little change in the conformational distribution of hexane in moving from the isotropic to the smectic phase by varying the density at constant temperature. In this case the increase in the anisotropic environment which favours conformations such as the all-*trans*, is balanced by an increase in density which favor conformations with more gauche links. Moving from the nematic to smectic phase by lowering the temperature generates a large increase in the number of all-*trans* configurations. The enhancement of *trans* conformations is more significant than would be predicted for an isolated hexane molecule with the same temperature change and there is considerable ordering induced by the smectic solvent. The scaled, simulated dipolar couplings, D_{ij} are in close agreement with the experimental data in the nematic phase, which demonstrates that the simulations are producing results which are similar to those of real systems.

The simulation results have been used to test three mean-field theories. For both nematic and smectic phases at $T^*=1.2$ the three models are equally successful in reproducing the overall features of the conformational distributions. At the lower temperature, the theoretical models are clearly underestimating the importance of the intermolecular contribution to the mean potential.

One possible criticism of an unusual solute–solvent system could be that it is too far removed from real systems, however, the ability to calculate dipolar couplings from the simulation data which match quite closely those observed on real solutions supports the view that this model is sufficiently close to reality to be a valuable means of exploring the behavior of flexible molecules in a liquid crystalline environment. This opens up the possibility of exploring the effects of changing solute structure on orientational order and conformational distributions in ordered liquid phases.

ACKNOWLEDGMENTS

We would like to thank Professor Alex Pines, University of California, Berkeley for many useful discussion. This work was performed under SERC grants GR/J72769 for staff and GR/J/74459 for computing hardware. J. A. would like to thank Conacyt (Mexico) and the British Council for a grant.

[1] J. W. Emsley and G. R. Luckhurst, Mol. Phys. **41**, 19 (1980).
[2] J. W. Emsley, G. R. Luckhurst, and C. P. Stockley, Proc. R. Soc. **381**, 117 (1982).
[3] M. R. Wilson and M. P. Allen, Mol. Cryst. Liquid Cryst. **198**, 465 (1991).
[4] S. T. W. Cheung and J. W. Emsley, Liquid Cryst. **13**, 265 (1993).

[5] C. J. R. Counsell, J. W. Emsley, G. R. Luckhurst, and H. S. Sachdev, Mol. Phys. **63**, 33 (1988).
[6] D. J. Photinos, E. T. Samulski, and H. Toriumi, J. Phys. Chem. **94**, 4694 (1990).
[7] M. E. Rosen, S. P. Rucker, C. Schmidt, and A. Pines, J. Phys. Chem. **97**, 3858 (1993).
[8] J. G. Gay and B. J. Berne, J. Chem. Phys. **74**, 3316 (1981).
[9] E. de Miguel, L-F. Rull, M. K. Chalam, and K. E. Gubbins, Mol. Phys. **74**, 405 (1991).
[10] W. E. Palke, J. W. Emsley, and D. J. Tildesley, Mol. Phys. **82**, 177 (1994).
[11] D. J. Adams, G. R. Luckhurst, and R. W. Phippen, Mol. Phys. **61**, 1575 (1987).
[12] G. R. Luckhurst, R. A. Stephens, and R. W. Phippen, Liquid Cryst. **8**, 451 (1989).
[13] J. W. Emsley, G. R. Luckhurst, W. E. Palke, and D. J. Tildesley, Liquid Cryst. **11**, 519 (1993).
[14] This result was generated using the programs CHARMM AND QUANTA. These programs have been developed by Molecular Simulations, Inc.
[15] J. P. Rykaert and A. Bellemans, Chem. Phys. Lett. **30**, 123 (1975).
[16] K. Singer, A. Taylor, and J. V. L. Singer, Mol. Phys. **33**, 1757 (1977).
[17] M. P. Allen and D. J. Tildesley, *Computer Simulation of Liquids* (Clarendon, Oxford, 1987).
[18] N. G. Almarza, E. Enciso, and M. J. Bermejo, J. Chem. Phys. **96**, 4625 (1992).
[19] M. Gochin, H. Zimmerman, and A. Pines, Chem. Phys. Lett. **137**, 51 (1987).
[20] A. J. van der Est, M. Y. Kok, and E. E. Burnell, Mol. Phys. **60**, 397 (1987).
[21] J. P. Straley, Phys. Rev. **10**, 1881 (1973).
[22] B. Janik, E. T. Samulski, and H. Toriumi, J. Phys. Chem. **91**, 1842 (1987).
[23] D. J. Photinos, E. T. Samulski, and H. Toriumi, J. Phys. Chem. **94**, 4688 (1990).
[24] S. Marcelja, J. Chem. Phys. **60**, 3599 (1974).
[25] D. J. Photinos, E. T. Samulski, and A. F. Terzis, J. Chem. Phys. **96**, 6979 (1992).